Excited-State Dynamics Leading either to Triplet Formation or Coordinative Expansion following Photolysis of Cu(II)-5,10,15,20-*meso-tetrakis*(phenyl)porphyrin or Cu(II)-5,10,15,20-*meso-tetrakis*(N-methylpyridium-4-yl)porphyrin: A DFT, TD-DFT, Luminescence and Femtosecond Time-Resolved Absorbance Study

Ross McGarry , Lazaros Varvarezos , Mary T. Pryce , Conor Long *

Posted Date: 24 July 2023

doi: 10.20944/preprints202307.1515.v1

Keywords: Porphyrin; Copper; Photophysics; DFT; TD-DFT; Luminescence; Transient Absorption; Femptosecond

Article

Excited-State Dynamics Leading either to Triplet Formation or Coordinative Expansion following Photolysis of Cu(II)-5,10,15,20-*meso*-*tetrakis*(phenyl)porphyrin or Cu(II)-5,10,15,20-*meso*-*tetrakis*(N-methylpyridium-4-yl)porphyrin: A DFT, TD-DFT, Luminescence and Femtosecond Time-Resolved Absorbance Study

Ross McGarry [1], Lazaros Varvarezos [2], Mary T. Pryce [1] and Conor Long [2,*]

[1] School of Chemical Sciences, Dublin City University, 9 Dublin, Ireland; ross.mcgarry6@mail.dcu.ie (R.M.); mary.pryce@dcu.ie (M.T.P.)
[2] School of Physical Sciences, Dublin City University, 9 Dublin, Ireland; varvarezos.lazaros@gmail.com
* Correspondence: conor.long@dcu.ie; Tel.:+353-1-7005503

Abstract: The photophysical properties of Cu(II) complexes with 5,10,15,20-*meso-tetrakis*(phenyl)porphyrin and 5,10,15,20-*meso-tetrakis*(*N*-methylpyridium-4-yl)porphyrin were examined by luminescence and femtosecond time-resolved absorbance methods respectively. These studies were supported by DFT and TD-DFT calculations which highlight the important role played by a ligand-to-metal charge-transfer states in directing the system towards either intersystem crossing to the triplet hypersurface or coordinative expansion to a five-coordinate quasi-stable intermediate. The latter processes occurs when the porphyrin is photolyzed in the presence of suitably located Lewis bases. Femtosecond time resolved absorbance measurements on Cu(II)-5,10,15,20-*meso-tetrakis*(*N*-methylpyridium-4-yl)porphyrin confirm that the coordinative expansion in water occurs in approximately 700 fs while crossing to the triplet hypersurface takes approximately 140 fs in the same solvent. These processes are mutually exclusive, but both can occur simultaneously depending on the environment of the porphyrin. The ratio of the two processes depends on the relative orientation of the Lewis base with respect to the copper atom at the time of excitation. As a consequence, copper porphyrins such as these, are excellent probes to the environment of the porphyrin, and can be used to identify the location of the porphyrin when interacting with DNA fragments.

Keywords: porphyrin; copper; photophysics; DFT; TD-DFT; luminescence; transient absorption; femptosecond

1. Introduction

There are numerous papers describing the photophysics and photochemistry of porphyrins with a wide variety of *meso*-substituents and in a wide range of solvent systems [1–12]. Copper-containing porphyrins are particularly interesting, with complex photophysical properties and they are amongst the most widely studied of the paramagnetic metalloporphyrins [13–47]. Given the broad range of systems studied, it is difficult to assign specific photophysical properties to specific substituent or solvent selections. As a result, we have decided to limit our investigations to two porphyrins, one the copper complex with 5,10,15,20-*meso-tetrakis*(phenyl)porphyrin (Figure 1a CuPh) and the second the copper complex with 5,10,15,20-*meso-tetrakis*(*N*-methylpyridium-4-yl)porphyrin (Figure 1b CuPy). CuPh is soluble in non-polar organic solvents such as toluene while CuPy, as its chloride salt, is soluble in water. We have also limited our investigations to these two solvents.

Preprints (www.preprints.org) | NOT PEER-REVIEWED | Posted: 24 July 2023 doi:10.20944/preprints202307.1515.v1

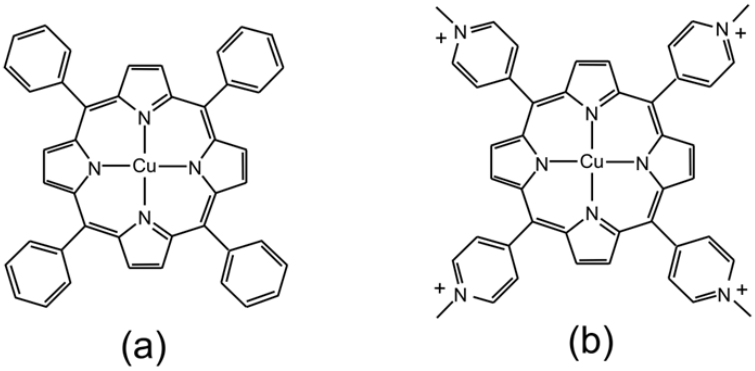

Figure 1. Representations of the molecular structures of (a) CuPh and (b) CuPy.

Copper porphyrins can exhibit characteristics of both porphyrin-centered or metal-centered excited-states and the coupling of porphyrin-based excited-states to the unpaired electron on the copper can, in specific circumstances, open an efficient spin-allowed route to the triplet hypersurface. This process known as Enhanced InterSystem Crossing (EISC) [48], and is represented schematically in Figure 2. Orbitals and electrons centered on the porphyrin are colored red, while those on the copper atom are colored blue. Of particular interest here is the role of the Ligand-to-Metal Charge Transfer (LMCT) state (green box) in facilitating a spin allowed route to the triplet hypersurface (dashed box).

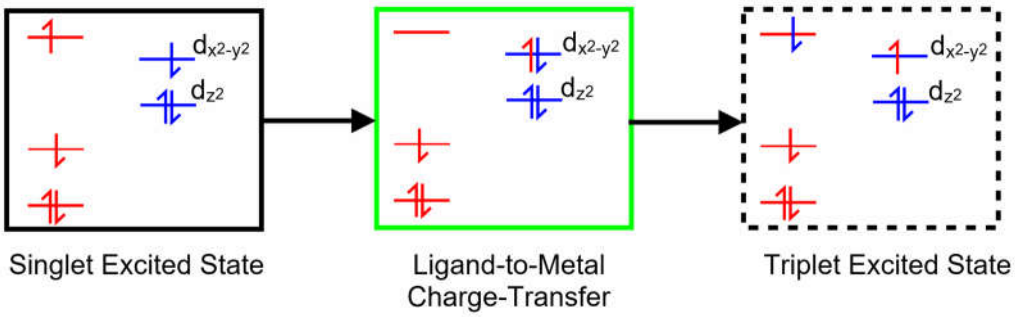

Figure 2. A schematic representation of a singlet excited-state of a copper porphyrin (black box), the Ligand-To-Metal Charge-Transfer State (green box) and a triplet excited-state (dashed box); red levels correspond to molecular orbitals located on the porphyrin with their electrons and blue levels represent orbitals on the copper atom with their electrons.

The efficiency and ultrafast nature of the EISC process has led researchers to assume that the photophysics of copper porphyrins is dominated by processes on the triplet hypersurface [49]. This includes the weak emission from CuPh in toluene solution which has been assigned to triplet states which are quenched by the addition of Lewis bases such as pyridine [49]. This was explained by proposing the formation of a five-coordinate complex by the reaction of the triplet excited-state(s) with a molecule of pyridine forming an exciplex i.e., a complex which exists in an electronic excited-state, but not in the ground-state [33,45,49–52].

Cationic water-soluble copper porphyrins such as CuPy have also been reported to form exciplexes with DNA bases, and for this reason they have used to probe a variety of DNA environments [16–19,33,39,53–56]. Studies in water usually use Raman spectroscopy and the expansion of the copper coordination sphere from four to five results in spectroscopic changes associated with porphyrin ring modes in the 1300-1700 Δcm^{-1} range. Unfortunately, Raman spectroscopy is insensitive to the nature of the fifth or axial ligand and it is only possible to distinguish between different axial ligands by measuring the lifetime of the five-coordinate species.

Preprints (www.preprints.org) | NOT PEER-REVIEWED | Posted: 24 July 2023 doi:10.20944/preprints202307.1515.v1

Luminescence techniques are of limited use in studying the photophysics of CuPy as it is non-emissive in water. However, emission is observed the presence of some DNA fragments, particularly those containing guanine-cytosine base-pairs such as the oligonucleotide $d(GC)_5$ [57]. It is assumed that the CuPy intercalates between the base pairs of the $d(GC)_5$ oligomer, and this prevents interaction between the copper atom and water molecules. This has the effect of "turning on" emission from, it is assumed, a triplet excited-state although the emission lifetime of 20 ns is rather short for phosphorescence.

In this work, the results of luminescence studies on CuPh in toluene are presented which are supported by DFT and TD-DFT calculations. In the case of CuPy, femtosecond TA experiments were performed either in pure water or in water containing $d(GC)_5$. In the first case, water can act both as a solvent medium but also as a potential axial ligand. In the second, water acts simply as a solvent but cannot act as an axial ligand. This allows the excited-state development to be monitored in an aqueous environment but in conditions where water has access to the copper atom and where it does not. DFT and TD-TDF calculations are then used to explain the experimental results.

These experiments were designed to answer several important questions. Firstly, it is unclear which excited-state or states react with the Lewis base to form the five-coordinate species. Most reports have assumed that it is the low-lying triplet states that are involved, although recent DFT studies have cast some doubt on this [39], as does the observation that the triplet state(s) can still be detected long after all the five-coordinate species have decayed [41]. Previous studies have attempted to provide plausible explanations for this particular observation but with limited success [16,41]. Secondly, there appears to be no plausible explanation as to why the lifetime of different five-coordinate complexes depends so markedly on the nature of the axial ligand. The complex with water has a lifetime of about 30 ps while the thymine complex survives into the nanosecond domain, despite both complexes involving oxygen donor atoms.

In this paper, the quantum chemical approach taken is to systematically investigate the effects of the location of Lewis bases close to the copper atom on excited-state development in CuPh and CuPy (the optimized coordinates for both porphyrins are presented in the Supplementary Materials in Table S1 and Table S2 respectively). Although this is a very computationally expensive approach it has the advantage that it does not rely on previous assumptions as to the multiplicity of the reactive excited-state(s). The results of these calculations are then compared to experimental results. This provides a clearer picture of the photophysics and photochemistry of copper porphyrins in general, and helps answer many of the outstanding questions which impact their use as probes in biological systems.

2. Results

Copper II complexes have an unpaired d-electron ($3d^9 4s^0$) which in the four-coordinate ground-state is presumed to be in the $d_{x^2-y^2}$ orbital. This d-configuration facilitates the location of the copper atom in the plane of the porphyrin ring, while the fully occupied d_{z^2} orbital inhibits axial coordination of further ligands. Optical excitation can populate either the S_1 or S_2 porphyrin-centered excited-states. The overall multiplicity of the copper porphyrin is that of a doublet, and Gouterman developed specific terminology to describe the electronic configuration or metalloporphyrins such as these [14]. A superscript numeral represents the overall multiplicity of the metal porphyrin complex, 2 for a doublet as is the case for the copper porphyrins, while the multiplicity of the porphyrin is indicated as an upper-case letter (S for singlet, D for Doublet and T for Triplet). The ordering of the states in terms of energy is represented by numeric subscripts. We have added a slight refinement by adding a subscript 4c and 5c to represent four-coordinate and five-coordinate complexes respectively. Schematic representations of these states are presented in Figure 3 which can act as a reference for the terminology used throughout this paper.

Preprints (www.preprints.org) | NOT PEER-REVIEWED | Posted: 24 July 2023 doi:10.20944/preprints202307.1515.v1

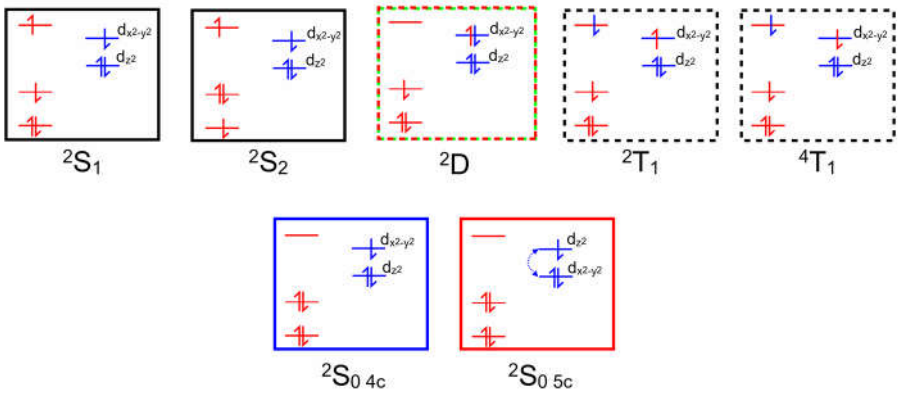

Figure 3. Schematic representations of the optically accessible states of copper porphyrins using the state assignments of Gouterman, the red levels/electrons are associated initially with the porphyrin, while the blue are associated with the copper atom, black boxes indicate S states, red/green dashed D (Ligand-to-Metal Charge-Transfer), black dashed T states, and blue and red indicate ground-states.

2.1. The Photophysical Properties of CuPh in Toluene

2.1.1. The Luminescence Studies

Outlined in Figure 4 are the absorption and emission data for CuPh in toluene solution at room temperature. The absorption spectrum is typical for this class of complex showing a sharp and intense B band absorption at 416 nm (ε = 2.796 × 105 m-1dm3cm-1) and a weaker Q band feature at 540 nm (1.25 × 104 m-1dm3cm-1). Excitation into either band results in a weak emission centered at 820 nm. The lifetime of this emission following 532 nm excitation is 30 ns. This emission lifetime was the same in oxygenated solvent as in degassed (freeze-pump-thaw) solution. The excitation spectrum for this emission has a profile, within experimental error, identical to the absorption spectrum (green dashed plot in Figure 4).

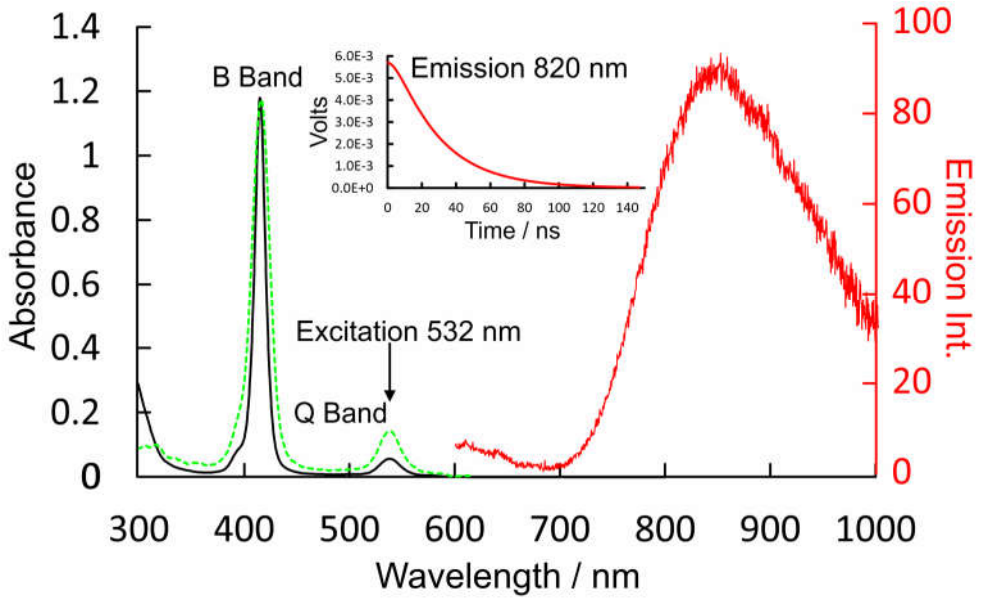

Figure 4. The UV/vis. absorption spectrum (black) showing the B and Q bands of CuPh in toluene, the emission (red) following 532 nm excitation and the time profile data for this emission as the insert, the dashed green spectrum is the excitation spectrum for the emission at 820 nm.

Preprints (www.preprints.org) | NOT PEER-REVIEWED | Posted: 24 July 2023 doi:10.20944/preprints202307.1515.v1

2.1.2. DFT and TD-DFT Calculations on CuPh in Toluene

Valence orbital energies and fragment compositions for CuPh are presented in Table S3 and a summary of electronic transitions are available in Table S4 in the Supplementary Materials. A relaxed potential energy plot was constructed by DFT methods, in which the location of a nitrogen atom of pyridine was held at fixed distances from the copper atom in CuPh. All other structural parameters were allowed to optimize in these calculations. The resulting plot of energy against Cu-*N*(pyridine) distances are presented in Figure 5 as the blue plot with data points indicated by blue squares. This profile exhibits a small minimum at a Cu-*N*(pyridine) distance of 2.5 Å which indicates very weak interaction between the copper porphyrin and pyridine. This weak interaction (see insert in Figure 5) results in a red-shift of the B band maximum [58], and will affect the time-averaged structure of the CuPh-pyridine complex in solution. It is estimated that between 35 and 55% of CuPh exists as the five-coordinate complex in neat pyridine at room temperature [50].

The ground-state coordinates obtained in the relaxed potential energy calculations were then used to estimate the energies of excited-states of all multiplicities (the unrestricted functional was used in these TD-DFT calculations) at all points along the reaction coordinate. These energies were then plotted against Cu-*N*(pyridine) distance. Only the three lowest energy states are presented in Figure 5 for clarity (plots of the 20 lowest energy excited-states are presented in the Supplementary Materials Figure S1). It is clear from these that neither the $^2T_1$ nor the $^4T_1$ states (dashed plots) interact significantly with pyridine. Of particular importance to this work is the relative energy of the Ligand-to-Metal Charge-Transfer state (^2D) (red curve) with respect to the triplet excited-states (electron density difference maps for the ^2D, $^2S_1$, and $^2S_2$ states are given in Figure S1, S3–S5 respectively). At all Cu-*N*(pyridine) distances, the ^2D state has lower energy than the $^2T_1$ state. It is clear from the work of Shafizadeh et al [59]. that the ^2D state is pivotal to determining if an efficient spin-allowed route exists for EISC to the triplet hypersurface. According to the calculations presented in Figure 5, crossing to the triplet surface would be energetically unfavorable and would therefore be, at best, a slow process for CuPh. Also notable is how the character of the ^2D state changes from LMCT to one which is more metal-centered when the Cu to *N*(Pyridine) distance is short (Figure 6). The electron density difference map on the left of Figure 6, i.e., where pyridine nitrogen is remote from the Cu atom, shows large blue volumes on the *meso*-carbons. This indicates that these carbons are involved substantially in the LMCT state. Any change to the nature of substituents on these *meso*-carbon atoms will, therefore, affect the energy of the ^2D state and consequently affect the photophysics of the porphyrin. If the Cu-*N*(pyridine) is short, the state is predominantly metal-centered, blue volumes are now evident on the copper atom indicating a significant d-d character in this state. This state then develops into the ground-state of the five-coordinate species $^2S_{0\ 5c}$. As indicated in Figure 5, this $^2S_{0\ 5c}$ state crosses to the $^2S_{0\ 4c}$ at very short Cu-*N*(pyridine) distances providing a rapid non-radiative return route to the four-coordinate complex via thermal ligand loss.

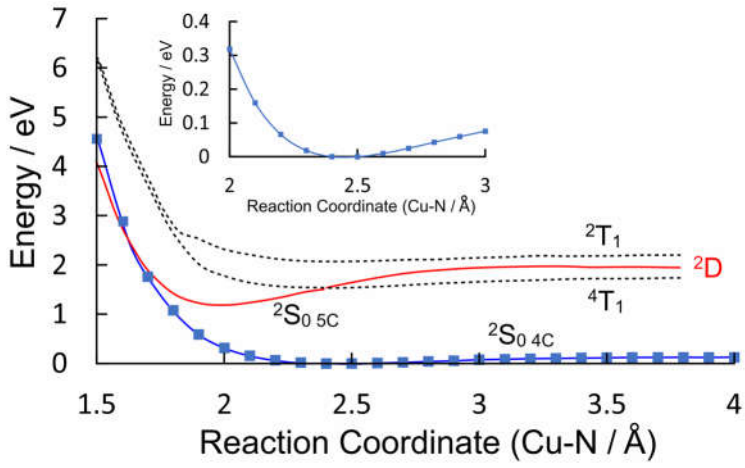

Preprints (www.preprints.org) | NOT PEER-REVIEWED | Posted: 24 July 2023 doi:10.20944/preprints202307.1515.v1

Figure 5. The potential energy profiles of the four-coordinate ground-state of CuPh ($^2S_{0\ 4C}$) as modelled in toluene versus the Cu-*N*(pyridine) distance (Å) (blue plot with data points indicated by blue squares); the $^2T_1$ and $^4T_1$ states are indicated by the dashed curves while the $^2D_0$ state is in red which develops into the $^2S_{0\ 5C}$ at short Cu-N distances.

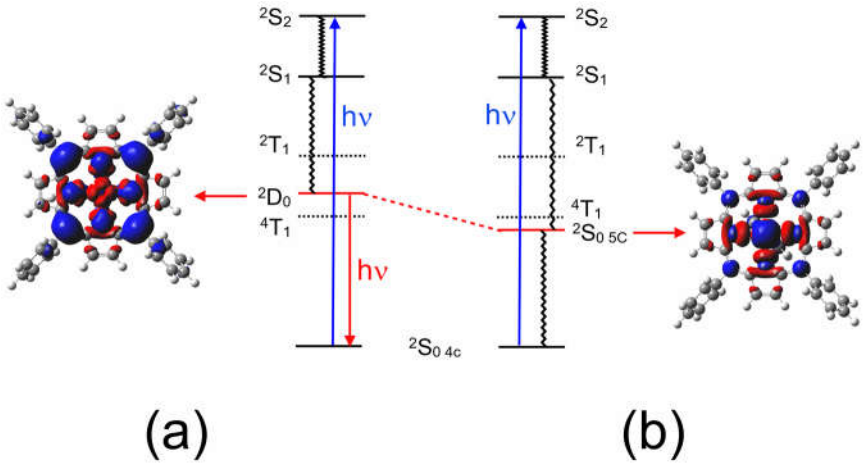

Figure 6. The development of the LMCT ($^2D_0$) state in CuPh as the Cu to *N*(pyridine) distance is reduced from (a) 3.5 to (b) 1.9 Å showing how it develops into a metal-centered state (the pyridine molecule is located on the far side of the porphyrin ring so that electron density changes on the copper atom can be viewed clearly) the blue volumes indicate the regions where the electron density is less in the ^2D or $^2S_{0\ 5c}$ state compared to the $^2S_{0\ 4c}$ state and the red volumes indicate the regions where the electron density increases (both electron density maps were cut at the same isovalue of 0.0004).

2.2. The Photophysical Properties of CuPy in Water

2.2.1. The UV/vis. Absorption of CuPy in Water

The UV/vis. spectrum of CuPy in water and water plus $d(GC)_5$ is presented in Figure 7 along with that of CuPh in toluene for comparison. This spectrum of CuPy is similar to that of CuPh except the absorption bands are broader, shifted to the red and much weaker. The B band maximum is at 424 nm ($\varepsilon = 9.5 \times 10^4$ $m^{-1}dm^3cm^{-1}$) compared to 416 nm for CuPh in toluene. This shift does have consequences for the fs-TA studies presented here which use the 2nd harmonic (400 nm) of the Ti:Sapphire fundamental as the pump pulse (upward arrow in Figure 7). This means that the excitation is to the high-energy side of the B band absorption where the CuPy has a relatively low extinction. For a given porphyrin, for example CuPh red shift of the B band results from changes to the porphyrin environment and can indicate coordination of a Lewis base to the copper center in the ground state. Such shifts have been used to estimate the equilibrium constants for these interactions [50]. Equally important for this work is the fact that the nature of the transition responsible for the B band changes in moving from CuPh to CuPy. For CuPh the transition is mainly porphyrin ring π-π* in character with some Metal-to-Ligand Charge-Transfer (MLCT) character (see Figure S6). For CuPy the B band transition has substantial intra-porphyrin character involving porphyrin ring-to-pyridinium charge transfer (Figure S7). Such a transition would be very sensitive to the polarity of the medium. This highlights the influence *meso*-substituents can exert on the photophysics of these porphyrins.

Preprints (www.preprints.org) | NOT PEER-REVIEWED | Posted: 24 July 2023 doi:10.20944/preprints202307.1515.v1

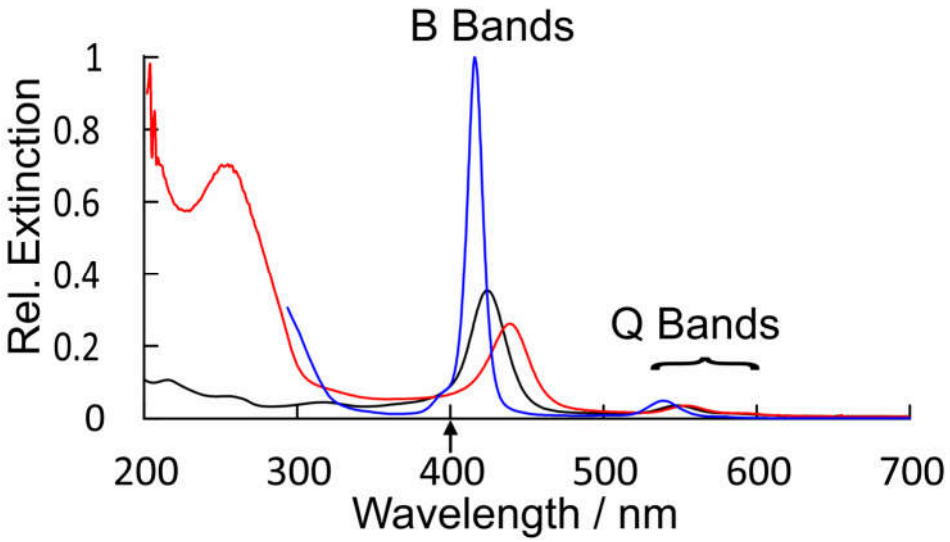

Figure 7. A comparison of the relative extinctions of CuPh in toluene (blue), CuPy in water (black), and CuPy plus $d(GC)_5$ in water (red) showing the broadening and red shifts of both the B bands and Q bands for CuPy in water and more particularly in water plus $d(GC)_5$, upward arrow indicates the fs TA pump wavelength.

2.2.2. DFT and TD-DFT Calculations on CuPy in Water

Valence orbital energies and fragment compositions for CuPy are presented in Table S5 and a summary of electronic transitions are available in Table S6 in the Supplementary Materials. Using the same approach as that for CuPh, relaxed potential energy profiles were constructed to model the excited-state development of CuPy in water and in the presence of three Lewis bases: pyridine, water, or thymine. Pyridine was chosen to allow a direct comparison with the results for the CuPh system described in Section 2.1.2, notwithstanding the fact that experimental verification for these results would be impossible because of solubility issues. Water and thymine were chosen because of reports in the literature that five-coordinate species form with these Lewis bases but they have very different lifetimes, 30 ps for water, while the thymine complex survives for many nanoseconds [17]. The potential energy plots for the three Lewis bases are presented in Figure 8.

Preprints (www.preprints.org) | NOT PEER-REVIEWED | Posted: 24 July 2023 doi:10.20944/preprints202307.1515.v1

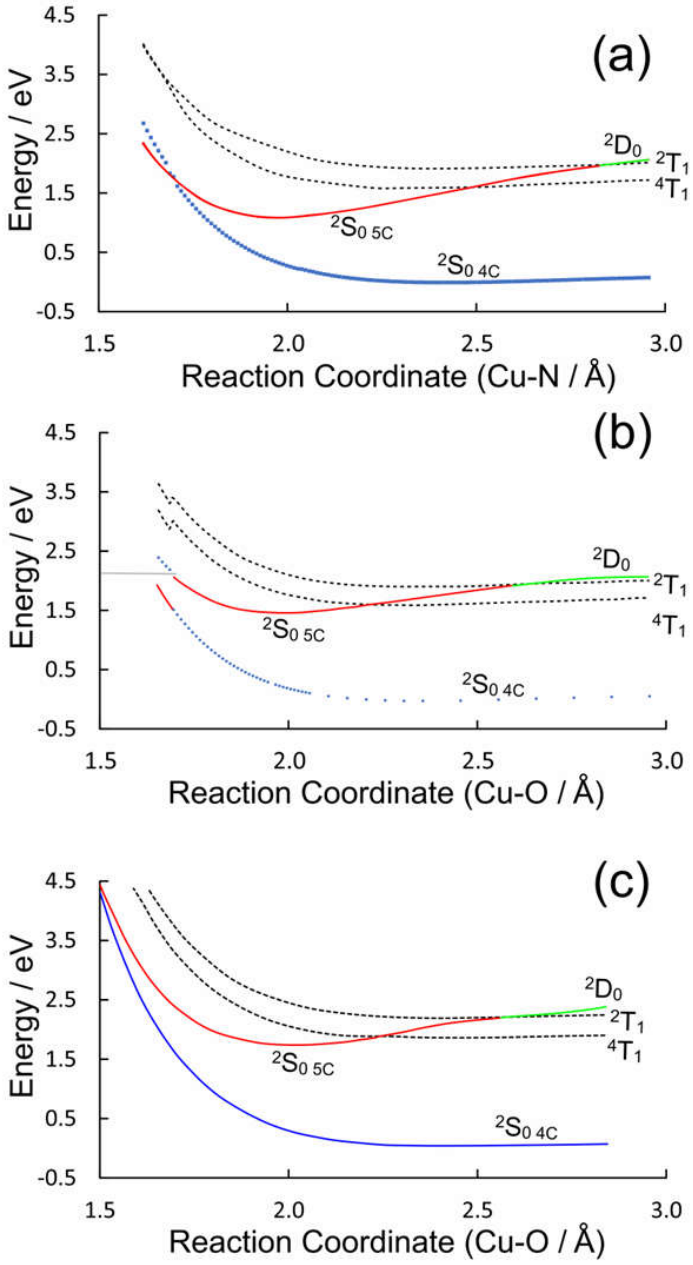

Figure 8. The potential energy plots obtained by varying the Cu-Donor Atom distance between 1.5 and 3 Å for (a) pyridine, (b) water, and (c) thymine; the blue plots describe the behavior of the four-coordinate $^2S_0$ ground-state the dashed curves represent the triplet $^2T_1$ and $^4T_1$ states and the green curve is the ^2D state which develops into the five-coordinate (5c) ground state ($^2S_{0\ 5c}$ red curve) at shorter Cu-donor atom distances.

The ground state potential energy curves are weakly binding in all three cases which indicates a very weak interaction between the copper atom and the Lewis bases. These plots present a broadly similar picture for the dependence of the excited-state energies with reaction coordinate but there are some subtle differences (see Figure S2). In all cases the triplet states ($^2T_1$ or $^4T_1$, dashed plots) do not interact significantly with the Lewis base. This is consistent with earlier DFT calculations which failed to detect any significant interactions between the triplet excited-states and an *O*-donor Lewis base [39]. Their energy profiles broadly follow those of the ground-state. Only one state ($^2S_{0\ 5C}$, red plot) presents a substantial energy minimum along the reaction coordinate for each Lewis base and at the energy minimum it has the properties of a ground-state species rather than an excited-state. If it were a ^2S excited-state it should be accompanied by a lower energy triplet state. No such state is evident

 doi:10.20944/preprints202307.1515.v1

from these calculations. For two of the three Lewis bases, pyridine or water, this $^2S_{0\ 5c}$ state crosses the four-coordinate $^2S_{0\ 4c}$ ground state at short Cu-Donor distances. This provides a facile route to relaxation to the pre-irradiated state. In the case of thymine however, the $^2S_{0\ 5c}$ complex is stabilized by an additional hydrogen bonding interaction between a porphyrin-ring nitrogen and an endocyclic hydrogen of the thymine, and in this case the $^2S_{0\ 5c}$ does not cross to the $^2S_{0\ 4c}$ state within the span of this reaction coordinate (see Tables S7 and S8). Consequently, no facile route to ligand-loss exists and the five-coordinate species will have a longer lifetime as measured by time-resolved Raman studies mentioned earlier [17].

2.3. Femtosecond Time-Resolved Absorbance Studies on CuPy in Aqueous Environments

The TA experiments described here can be divided into two classes. In the first, water acts as more than just a solvent, it also acts as a Lewis base towards the copper center. In the second, water simply acts as the solvent, $d(GC)_5$ is added to prevent water acting as a Lewis base as the copper porphyrin is intercalated between the GC base pairs and held in a hydrophobic environment [60]. In this way it is possible to highlight the effect that *meso*-pyridinium-4-yl substituents, as opposed to phenyl substituents, have on the on the excited-state formation and dynamics. Experiments in pure water highlight the additional role of water as a Lewis base.

2.3.1. Femtosecond Time-Resolved Absorbance Studies on CuPy in Water

The UV/vis. changes observed following pulsed photolysis ($\lambda_{exc.}$ = 400 nm) of a 0.05 mM solution of CuPy in pure water are presented in Figure 9a. These are difference spectra, where the negative absorbances represent the bleaching of the parent absorptions upon excitation, for instance the B band features at 424 nm and the weak Q band at 548 nm. An intense product band is formed within the excitation pulse ca 468 nm with very weak features in the visible region the most intense of which is at 700 nm (see inset). Over the initial 700 fs this feature decays and the absorbance at 460 nm becomes more intense and narrows. The parent bleach also appears to recover. This recovery signal is deceptive however, as it corresponds to the development of the overlapping absorbance at 460 nm rather than the reformation of the parent complex. As the product absorption occurs immediately to the red of the ground-state bleach results in a so-called derivative-like difference spectrum which is characteristic of the formation of a five-coordinate species [61].

2.3.2. Femtosecond Time-Resolved Absorbance Studies on CuPy in Water Plus $d(GC)_5$

The UV/vis. changes observed following pulsed photolysis ($\lambda_{exc.}$ = 400 nm) of a 0.05 mM solution of CuPy in a buffered (pH 7.0) aqueous solution containing 0.1 mM $d(GC)_5$ are presented in Figure 9b. The parent bleach is observed at 430 nm, and it is important to note, this bleach does not recover in the timescale of this experiment (2.1 ps). A broad product absorption is evident at 485 nm which changes little. Those minor changes are highlighted with arrows in Figure 9b. However, a significant and broad absorption was observed in the 650 to 800 nm region. This region is known to provide more diagnostic information on the nature of excited-state species in metalloporphyrin systems [61]. The features in the 400-600 nm region are insensitive to the nature of the excited-states involved. The broad absorption in the red region (monitored at 783 nm) decays on the ultrafast timescale with a lifetime of approximately 140 fs, close to the response time of the experimental setup estimated to be 90 fs. No recovery of the parent bleach was observed in this timescale. The product absorbance in the 400 to 600 nm region therefore represents the sequential formation of ^2S, ^2D and ^2T excited-states all of which have similar absorbances in this region [16,61]. The ultimate product is the $^2T_1$ state which is thought to establish an equilibrium with the $^4T_1$ state [50].

Preprints (www.preprints.org) | NOT PEER-REVIEWED | Posted: 24 July 2023 doi:10.20944/preprints202307.1515.v1

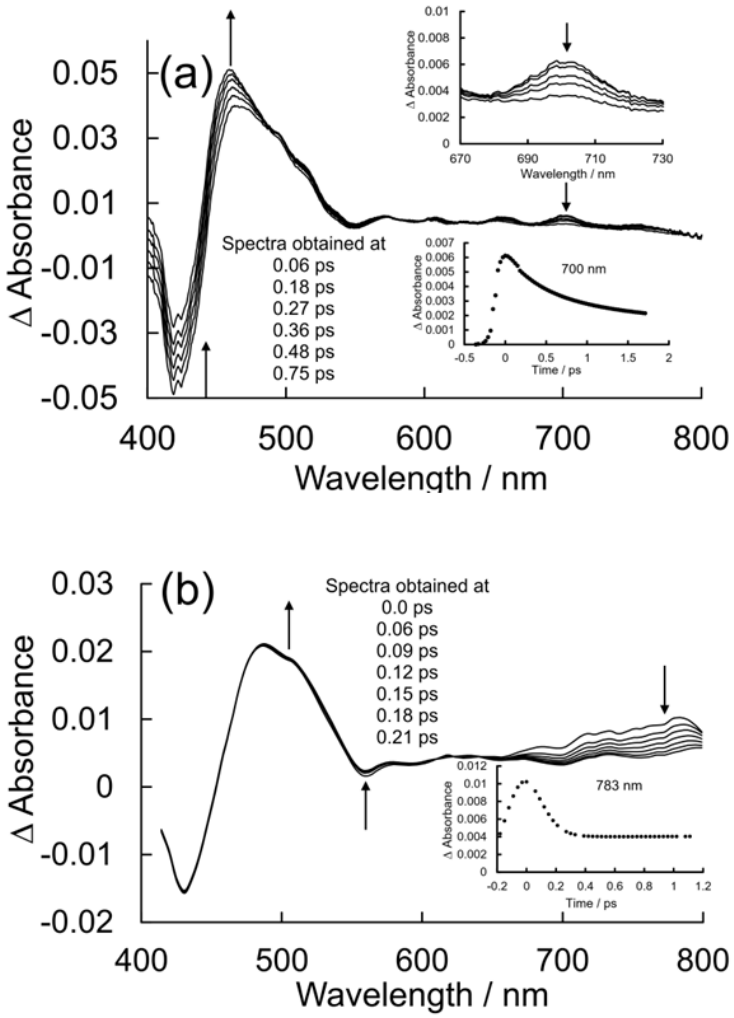

Figure 9. (a) The absorbance changes observed following 400 nm pulsed excitation of CuPy in pure water showing changes consistent with the formation of a five-coordinate species in 700 fs, the insert shows the temporal evolution of the weak feature at 700 nm; (b) the absorbance changes observed following 400 nm pulsed excitation of CuPy in water with added d(GC)$_5$ showing changes consistent with the formation of a triplet excited-state and a precursor state with a broad absorbance between 700 and 800 nm which decays in 140 fs (see inset).

3. Discussion

The elegant work of Shafizadeh [48,59], highlighted the central role of the porphyrin-to-metal charge-transfer (^{2}D) states in the rapid formation of triplet excited-states in copper porphyrins. However, for this to occur the ^{2}D state must lie at higher energy to the $^2T_1$ state (Figure 10). The calculations presented in Figure 5 clearly indicate that for CuPh in toluene, the $^2D_0$ state lies below the $^2T_1$ state at all Cu-*N*(pyridine) distances, and therefore the $^2T_1$ state is unlikely to be populated in this system [49]. Consequently, the weak emission observed in toluene solution probably originates in the ^{2}D state (Figure 6a). This explains why the emission lifetime measured in this work is relatively short (30 ns) and insensitive to the presence of triplet quenchers such as molecular oxygen.

The insert in Figure 5 clearly indicates that there is a weak interaction between the copper atom and a pyridine molecule in the ground-state. Therefore, the probability that a pyridine molecule will be positioned correctly to coordinate to the copper atom at any given time will be directly dependent on the pyridine concentration. It has been noted previously that the correct orientation of the porphyrin relative to the Lewis base is essential for the coordinative expansion to occur [54]. This interaction with pyridine alters the formal d electron configuration on the copper. This prevents the formation of the emissive state (^{2}D) and therefore will manifest as a diffusive quenching despite the

Preprints (www.preprints.org) | NOT PEER-REVIEWED | Posted: 24 July 2023 doi:10.20944/preprints202307.1515.v1

excited-state development occurring too fast for diffusion to play a role. Figure 6 shows the transformation of the ^2D state to the $^2S_{0\ 5c}$ state where the electron configuration on the copper changes to accommodate the electron donation from the pyridine ligand into the d_{z2} orbital on the copper. This configuration change is accompanied by a structural change for the porphyrin with the copper atom being displaced from the porphyrin plane to form the so-called "domed" structure (Figure 11). This quasi-stable species then ejects the axial pyridine ligand in a thermal process regenerating the four-coordinate ground-state.

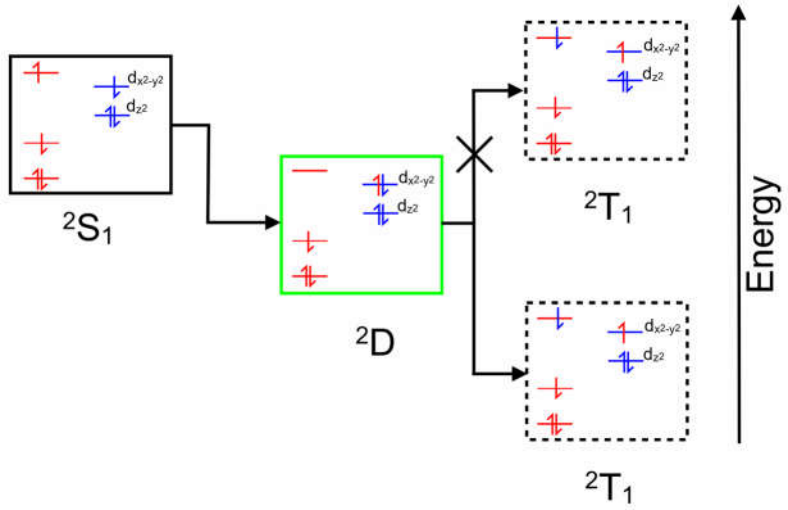

Figure 10. A schematic representation of the EISC to the $^2T_1$ state where the $^2T_1$ energy is less than that of the ^2D state, while no such crossing occurs if the $^2T_1$ energy is greater than the ^2D energy.

Turning to the CuPy system, the relaxed potential energy plots in Figure 8 exhibit one significant difference compared to the plot for the CuPh system (Figure 5). The ^2D state lies at higher energy to the $^2T_1$ state for large Cu-donor atom distances (green plot segments). This means that in the absence of Lewis bases or in situations where the Lewis base is not correctly located to coordinate the copper atom, excitation into either the $^2S_2$ or $^2S_1$ state will rapidly populate to the ^2D state which in turn will cross to the $^2T_1$ state (Figure 9b). At shorter Cu-to-donor atom distances and where the Lewis base is correctly orientated to coordinate to the copper atom, the ^2D state falls below the $^2T_1$ state which inhibits off crossing to the $^2T_1$ state (red plot segments). The system then forms the quasi-stable five-coordinate species by relaxing into the $^2S_{0\ 5c}$ potential minimum, a process which takes some 700 fs in water (Figure 9a). This process is slower (700 fs) than the formation of the triplet state (140 fs). This means that the formation of the five-coordinate species depends, not so much on the concentration of the Lewis base, but on the probability that the Lewis base is correctly orientated to act as a ligand to the copper atom at the instant of excitation. This in turn explains why the triplet excited-state is detected even after the five-coordinate species has relaxed the four-coordinate species. In pure water approximately 5% of the copper porphyrin molecules are not orientated correctly for water to act as ligand to the copper atom at any given time. This results in a 5% yield of the triplet excited-states even in pure water [41]. The five-coordinate species formed cannot be formally classified as an exciplex because it is formed in its lowest energy state. Water is then expelled from the adduct regenerating the four-coordinate species in about 30 ns.

The rate of expulsion of the axial ligand from the five-coordinate species depends on the nature of the axial ligand. For example, the rate is relatively slow when thymine is the axial ligand. This is because for thymine, additional hydrogen bonding interactions between the endocyclic hydrogen atoms and the nitrogen atoms of the porphyrin stabilizes this species (Figure 11a). The copper atom is displaced from the center of the porphyrin ring because of alterations to the d electron configuration (Figure 11b). The porphyrin ring vibrations are insensitive to the nature of the axial ligand and it is the changes to these vibrations which are monitored in Raman studies in the 1300 to

Preprints (www.preprints.org) | NOT PEER-REVIEWED | Posted: 24 July 2023 doi:10.20944/preprints202307.1515.v1

1700 Δcm^{-1} region. This explains why simple Raman spectroscopy cannot distinguish between different five-coordinate complexes and time-resolved Raman techniques are required.

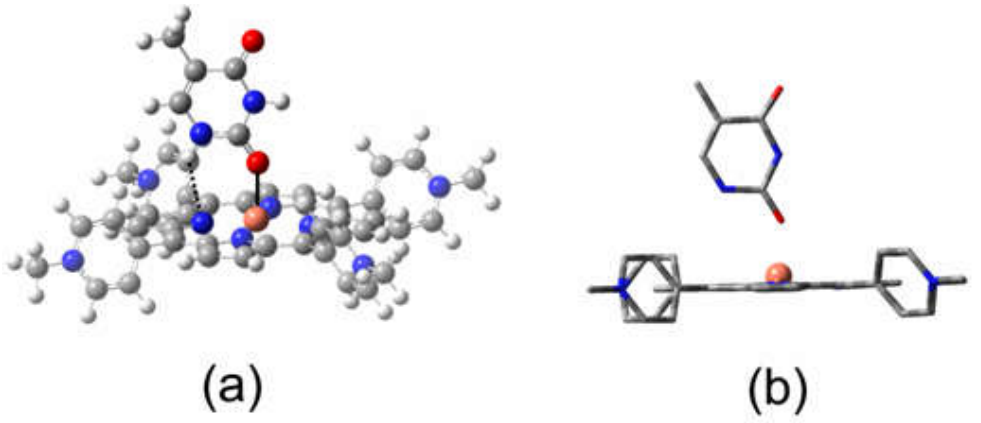

Figure 11. (a) A representation of the CuPy-thymine interaction at a Cu-O(thymine) distance of 2.145 Å in CuPy showing the Cu-O interaction as a solid black bond and the additional endocyclic hydrogen to porphyrin nitrogen hydrogen bonding interaction as a black dashed bond), most porphyrin atoms are rendered opaque for clarity (b) a side-on view of CuPy (wire frame, hydrogen atoms removed for clarity) showing the displacement of the copper atom from the plane of the porphyrin ring (the optimized structure was obtained using a ub3lyp/lanl2dz model chemistry.

4. Materials and Methods

4.1. Transient Absorption (TA) Spectroscopy

The ultrafast (fs) transient absorption spectroscopy (UTAS) measurements reported in this work, were performed using a Newport Transient Absorption Spectrometer. The spectral resolution of the system is ca. 2 nm. The laser pulses were delivered by a 1 kHz Coherent Astrella Ti:Sapphire laser system with ~40 fs pulse duration (measured by an autocorrelator) at a repetition rate of 1 kHz and a wavelength centered at 800 nm. Second harmonic radiation, at 400 nm, provided the pump beam, and the incident laser energy on the sample was ca. 3 μJ. The white light continuum (330-900 nm) generated by means of a CaF_2 crystal, served as the probe beam. The experiments were performed at a magic angle between the polarization of the pump beam and that of the probe continuum with a spot size in the range 150 to 200 μm. The temporal resolution of the UTAS system was estimated to be ~ 120 fs and the instrument response function is approximately 90 fs.

4.2. Luminescence Studies

Time-resolved emission spectroscopy was carried out using an LP980 spectrometer (Edinburgh Instruments UK) coupled with a Quantel Q-smart 450 YAG laser, producing the second harmonic of the fundamental at 532 nm (8 mJ per pulse). The absorbance of the sample solution was adjusted to ca. 0.2 at 532 nm in spectroscopy grade toluene (Merck Life Science Ltd.) and was monitored throughout the experiment. There was no evidence for sample photodegradation in these experiments.

4.3. Materials

Copper(II)-*meso-tetrakis*(N-methyl-pyridinium-4-yl)porphine tetrachloride and Copper(II)-5,10,15,20- *meso-tetrakis*(phenyl)porphyrin were purchased from PorphyChem SAS. CuPh was further purified by silica gel column chromatography (3:1 Pentane:dichloromethane). The oligonucleotide $d(GC)_5$ was received as a gift from Professor Susan Quinn, University College Dublin having been purchased from Eurogentex.

 doi:10.20944/preprints202307.1515.v1

4.4. Sample Preparation

UV-vis and emission spectroscopy were recorded using a Horiba Duetta Fluorescence and Absorbance spectrometer. Solutions were prepared in a 1 cm quartz fluorescence cuvette, using spectroscopy grade Toluene (Merck Life Science Ltd.) or Deuterium oxide 99.90% (Eurisotop). Samples for fs transient spectroscopy measurements were prepared in a demountable liquid cell (Harrick Scientific Products Inc., New York) with two 25 mm (2 mm thickness) CaF_2 windows (Crystran Ltd., UK) using a 500 μm PTFE spacer. A Fisherbrand CTP100 peristatic pump was used to flow the sample during the time resolved measurements. The CuPy samples were prepared in 18.2 MΩ MilliQ water or a 50 mM phosphate buffer (pH = 7) in D_2O.

4.5. Computational Methods

All Density Functional Theory (DFT) calculations were performed using the Gaussian 16, Revision B.01 program suite [62]. The unrestricted hybrid density functional UB3LYP was used in the majority of calculations [63,64]. All calculations used the double zeta quality LanL2DZ basis set which has proved successful at modelling other inorganic systems at moderate computational cost [65–67]. Structures were optimized to tight convergence criteria with the exception that the pyridinium methyl groups were, when required, frozen in the latter stages of the optimization to prevent convergence problems caused by the freely rotating methyl groups. A doublet ground-state multiplicity and an overall charge of zero for the CuPh porphyrin and +4 for the CuPy porphyrin was used. The nature and energy of higher energy states were calculated using Time-Dependent Density Functional Theory (TD-DFT) methods [68–73]. Calculations were modelled for the presence of toluene in the case of CuPh and water in the case of CuPy using the Polarizable Continuum Model [74,75]. GaussView (revision 6.0.16) was used to visualize the results of quantum calculations [76].

5. Conclusions

These results highlight the important role of a charge-transfer state in directing the photophysics of copper porphyrins. Both solvent and the nature of substituents on the porphyrin *meso*-positions can affect the energy of this state and therefore can change the direction of the excited-state development. It is incorrect to assume that a porphyrin with *meso*-phenyl substituents will behave in a similar way to porphyrins containing *meso*-pyridinium groups. Solvents can affect the photophysics of these porphyrins by altering the energy of the ^2D ligand-to-metal charge-transfer state through changes to the medium polarity, but also by their Lewis base character. For the CuPy system, the presence of a Lewis base donor atom close to the copper atom can divert the system away from crossing to the triplet surface by opening a route to coordinative expansion. This forms a ground-state five-coordinate species. Both triplet formation and coordinative expansion occur on the ultrafast timescale 140 fs and 700 fs respectively, too fast for bimolecular diffusion to play a significant role. Consequently, copper porphyrins are excellent probes for the immediate environment of the copper atom at the instant of excitation. Figure 12 summarizes the excited-state development of these copper porphyrin systems.

Preprints (www.preprints.org) | NOT PEER-REVIEWED | Posted: 24 July 2023 doi:10.20944/preprints202307.1515.v1

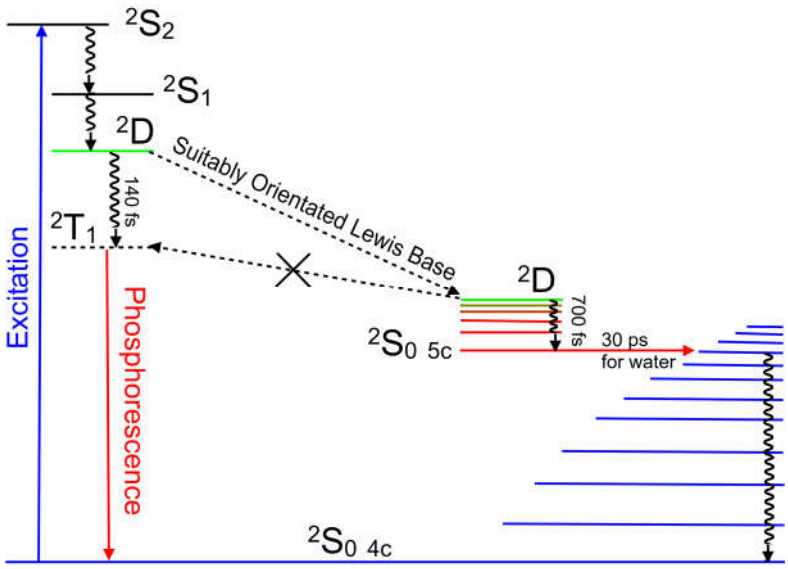

Figure 12. An energy level representation of the photophysical processes following 400 nm excitation of CuPy describing the population of the $^2T_1$ state in the absence of a suitably orientated Lewis base while the five-coordinate species provides a deactivation route to the four-coordinate species.

Supplementary Materials: The following supporting information can be downloaded at the website of this paper posted on Preprints.org, Table S1. Optimized atomic coordinates of the CuPh in toluene; Table S2. Optimized atomic coordinates of the CuPy in water; Table S3. Valence orbitals with fragment contributions (%) for CuPh; Table S4. Summary of calculated electronic transitions for CuPh; Table S5. Orbital Fragment contributions (%) for CuPy; Table S6. Summary of calculated electronic transitions for CuPy; Table S7. Optimized atomic coordinates for CuPy-thymine; Table S8. Optimized Bond-Lengths and Angles for CuPy-thymine; Figure S1. The adiabatic plots for the lowest 20 excited states along the Cu-N(pyridine) reaction coordinate; Figure S2. The adiabatic plots for the lowest 20 excited states along the Cu-O(water) reaction coordinate; Figure S4. The electron density difference maps the Q band excited-states; Figure S5. The electron density difference maps for the B band excited states.

Author Contributions: Conceptualization, C.L.; methodology, C.L. and M.T.P.; software, C.L., L.V., R.M.; validation, C.L., R.M. and V.L.; formal analysis, C.L., L.V., R.M. and M.T.P.; investigation, C.L., L.V. and R.M.; resources, M.T.P.; data curation, C.L.; writing—original draft preparation, C.L.; writing—review and editing, C.L., R.M., L.V. and M.T.P.; visualization, R.M, L.V., C.L. and M.T.P.; supervision, C.L and M.T.P.; project administration, C.L. and M.T.P.; funding acquisition, M.T.P. and C.L. All authors have read and agreed to the published version of the manuscript.

Funding: This research was funded by Science Foundation Ireland (SFI) under grants 19/FFP/6882, 19/FFP/6956, 16/RI/3696, and 22/NCF/TF/10998. Funding was also provided by the Sustainable Energy Authority of Ireland under the SEAI National Energy Research, Development & Demonstration Funding Programme 18/RDD/282.

Acknowledgments: The authors thank the DJEI/DES/SFI/HEA Irish Centre for High-End Computing (ICHEC) for the provision of computational facilities.

Conflicts of Interest: The authors declare no conflict of interest. The funders had no role in the design of the study; in the collection, analyses, or interpretation of data; in the writing of the manuscript; or in the decision to publish the results.

References

1. Boyle, N.M.; Rochford, J.; Pryce, M.T., Thienyl-Appended porphyrins: Synthesis, photophysical and electrochemical properties, and their applications. *Coord. Chem. Rev.* **2010,** 254, 77–102, https://10.1016/j.ccr.2009.09.001.
2. O'Neill, J.S.; Kearney, L.; Brandon, M.P.; Pryce, M.T., Design components of porphyrin-based photocatalytic hydrogen evolution systems: A review. *Coord. Chem. Rev.* **2022,** 467, https://10.1016/j.ccr.2022.214599.

3. O'Neill, J.S.; Boyle, N.M.; Passos, T.M.; Heintz, K.; Browne, W.R.; Quilty, B.; Pryce, M.T., Photophysical and electrochemical properties of meso-tetrathien-2 '-yl porphyrins compared to meso-tetraphenylporphyrin. *J. Photochem. Photobiol., A* **2023,** 438, https://10.1016/j.jphotochem.2023.114573.
4. Rochford, J.; Botchway, S.; McGarvey, J.J.; Rooney, A.D.; Pryce, M.T., Photophysical and Electrochemical Properties of meso-Substituted Thien-2-yl Zn(II) Porphyrins. *J. Phys. Chem. A* **2008,** 112, 11611–11618, https://10.1021/jp805809p.
5. Bram, O.; Cannizzo, A.; Chergui, M., Ultrafast Broadband Fluorescence Up-conversion Study of the Electronic Relaxation of Metalloporphyrins. *J. Phys. Chem. A* **2019,** 123, 1461–1468, https://10.1021/acs.jpca.9b00007.
6. Yu, H.Z.; Baskin, J.S.; Zewail, A.H., Ultrafast dynamics of porphyrins in the condensed phase: II. Zinc tetraphenylporphyrin. *J. Phys. Chem. A* **2002,** 106, 9845–9854, https://10.1021/jp0203999.
7. Parson, W.W., Electron-Transfer Dynamics in a Zn-Porphyrin-Quinone Cyclophane: Effects of Solvent, Vibrational Relaxations, and Conical Intersections. *J. Phys. Chem. B* **2018,** 122, 3854–3863, https://10.1021/acs.jpcb.8b01072.
8. Horvath, O.; Valicsek, Z.; Harrach, G.; Lendvay, G.; Fodor, M.A., Spectroscopic and photochemical properties of water-soluble metalloporphyrins of distorted structure. *Coord. Chem. Rev.* **2012,** 256, 1531–1545, https://10.1016/j.ccr.2012.02.011.
9. Lopes, J.M. S.; Sampaio, R.N.; Ito, A.S.; Batista, A.A.; Machado, A.E. H.; Araujo, P.T.; Neto, N.M. B., Evolution of electronic and vibronic transitions in metal(II) meso-tetra(4-pyridyl)porphyrins. *Spectrochimica Acta Part a-Molecular and Biomolecular Spectroscopy* **2019,** 215, 327–333, https://10.1016/j.saa.2019.02.024.
10. Rury, A.S.; Sension, R.J., Broadband ultrafast transient absorption of iron (III) tetraphenylporphyrin chloride in the condensed phase. *Chem. Phys.* **2013,** 422, 220–228, https://10.1016/j.chemphys.2013.01.025.
11. Inamo, M.; Okabe, C.; Nakabayashi, T.; Nishi, N.; Hoshino, M., Femtosecond time-resolved photo-absorption studies on the excitation dynamics of chromium(III) porphyrin complexes in solution. *Chem. Phys. Lett.* **2007,** 445, 167–172, https://10.1016/j.cplett.2007.07.079.
12. Velate, S.; Liu, X.; Steer, R.P., Does the radiationless relaxation of Soret-excited metalloporphyrins follow the energy gap law? *Chem. Phys. Lett.* **2006,** 427, 295–299, https://10.1016/j.cplett.2006.06.119.
13. Yeon, K.Y.; Jeong, D.; Kim, S.K., Intrinsic lifetimes of the Soret bands of the free-base tetraphenylporphine (H2TPP) and Cu(II)TPP in the condensed phase. *Chem. Commun.* **2010,** 46, 5572–5574, https://10.1039/c0cc01115k.
14. Gouterman, M.; Mathies, R.A.; Smith, B.E.; Caughey, W.S., Porphyrins 19. Tripdoublet and Quartet Luminescence in Cu and VO Complexes. *J. Chem. Phys.* **1970,** 52, 3795–+, https://10.1063/1.1673560.
15. Magde, D.; Windsor, M.W.; Holten, D.; Gouterman, M., Picosecond Flash-Photolysis - Transient Absorption in Sn(IV), Pd(II) and Cu(II) Porphyrins. *Chem. Phys. Lett.* **1974,** 29, 183–188, https://10.1016/0009-2614(74)85008-6.
16. Chirvony, V.S.; Galievsky, V.A.; Sazanovich, I.V.; Turpin, P.Y., Dynamics of formation and decay of the exciplex created between excited Cu(II)-5,10,15,20-tetrakis(4-N-methylpyridyl)porphyrin and thymine C=O groups in short oligothymidylates and double-stranded [poly(dA–dT)]2. *J. Photochem. Photobiol., B* **1999,** 52, 43–50.
17. Kruglik, S.G.; Mojzes, P.; Mizutani, Y.; Kitagawa, T.; Turpin, P.-Y., Time-Resolved Resonance Raman Study of the Exciplex Formed between Excited Cu-Porphyrin and DNA. *J. Phys. Chem. B* **2001,** 105, 5018–5031.
18. Turpin, P.Y.; Chinsky, L.; Laigle, A.; Tsuboi, M.; Kincaid, J.R.; Nakamoto, K., A Porphyrin-DNA Exciplex: Resonance Raman Spectra of Electronically Excited Cu(TMpy-P4) Bound to Poly(dA-dT).Poly(dA-dT). *Photochem. Photobiol.* **1990,** 51, 519–525, https://10.1111/j.1751-1097.1990.tb01960.x.
19. Mojzes, P.; Praus, P.; Baumruk, V.; Turpin, P.Y.; Matousek, P.; Towrie, M., Structural features of two distinct molecular complexes of copper(II) cationic porphyrin and deoxyribonucleotides. *Biopolymers* **2002,** 67, 278–281.
20. Novy, J.; Urbanova, M., Vibrational and electronic circular dichroism study of the interactions of cationic porphyrins with (dG-dC)(10) and (dA-dT)(10). *Biopolymers* **2007,** 85, 349–358, https://10.1002/bip.20654.
21. Gaier, A.J.; McMillin, D.R., Binding Studies of G-Quadruplex DNA and Porphyrins: Cu(T4) vs Sterically Friendly Cu(tD4). *Inorg. Chem.* **2015,** 54, 4504–4511, https://10.1021/acs.inorgchem.5b00340.
22. Xu, Z.M.; Swavey, S., Photoinduced DNA binding of a multi-metallic (Cu(II)/Ru(II)/Pt(II)) porphyrin complex. *Inorg. Chem. Commun.* **2011,** 14, 882–883, https://10.1016/j.inoche.2011.03.017.
23. Vashurin, A.S.; Pukhovskaya, S.G.; Garasko, E.V.; Voronina, A.A.; Golubchikov, O.A., Formation and Bacteriostatic Properties of AgII and Cu-II Complexes of meso-Tetrakis(N-methyl-4-pyridyl)-porphyrin Tetratosylate. *Macroheterocycles* **2014,** 7, 272–275, https://10.6060/mhc140491v.
24. Lee, M.J.; Lee, G.J.; Lee, D.J.; Kim, S.K.; Kim, J.M., Interaction of Cu(II)-meso-tetrakis(n-N-methylpyridiniumyl)porphyrin (n=2,3,4) with native and synthetic polynucleotides probed by polarized spectroscopy. *Bull. Korean Chem. Soc.* **2005,** 26, 1728–1734.

25. Monaselidze, J.R.; Kiladze, M.T.; Gorgoshidze, M.Z.; Khachidze, D.G.; Bregadze, V.G.; Lomidze, E.M.; Lezhava, T.A., Microcalorimetric study of DNA-Cu(II)TOEPyP(4) porphyrin complex. *J. Therm. Anal. Calorim.* **2012,** 108, 127–131, https://10.1007/s10973-011-1669-4.
26. Li, J.; Wei, Y.L.; Guo, L.M.; Zhang, C.H.; Jiao, Y.; Shuang, S.M.; Dong, C., Study on spectroscopic characterization of Cu porphyrin/Co porphyrin and their interactions with ctDNA. *Talanta* **2008,** 76, 34–39, https://10.1016/j.talanta.2008.01.065.
27. Barkhudaryan, V.G.; Ananyan, G.V., Development of viscometric methods for studying the interaction of various porphyrins with DNA. Part II: Meso-tetra-(3N-hydroxyethylpyridyl) porphyrin and its Ni-, Cu-,Co -and Zn-containing derivatives. *J. Porphyrins Phthalocyanines* **2016,** 20, 766–772, https://10.1142/s1088424616500668.
28. Tears, D.K. C.; McMillin, D.R., Duplex hydrogen banding promotes intercalation of Cu(T4) in DNA hairpins (Cu(T4) = meso-tetrakis(4-(N-methylpyridyl))porphyrincopper(II)). *Chem. Commun.* **1998**, 2517-2518.
29. Avetisyan, A.A.; Vardanyan, I.V.; Dalyan, Y.B., Thermodynamics of interaction of meso-tetra-(4N-oxyethylpyridyl) porphyrin and its Cu(II)- and Co(II)-containing derivatives with A and B forms of DNA. *J. Porphyrins Phthalocyanines* **2017,** 21, 731–738, https://10.1142/s1088424617500742.
30. Xu, Z.M.; Swavey, S., Light induced photoreactions with plasmid DNA by Cu/Ru and Cu/Ru/Pt multi-metallic porphyrins. *Dalton Trans.* **2011,** 40, 7319–7326, https://10.1039/c1dt10350d.
31. Nguyen, T.; Hakansson, P.; Edge, R.; Collison, D.; Goodman, B.A.; Burns, J.R.; Stulz, E., EPR based distance measurement in Cu-porphyrin-DNA. *New J. Chem.* **2014,** 38, 5254–5259, https://10.1039/c4nj00673a.
32. Pasternack, R.F.; Gibbs, E.J.; Gaudemer, A.; Antebi, A.; Bassner, S.; Depoy, L.; Turner, D.H.; Williams, A.; Laplace, F.; Lansard, M.H.; Merienne, C.; Perreefauvet, M., Molecular-Complexes of Nucleosides and Nucleotides with a Monomeric Cationic Porphyrin and some of its Metal Derivatives. *J. Am. Chem. Soc.* **1985,** 107, 8179–8186, https://10.1021/ja00312a061.
33. Kruglik, S.G.; Apanasevich, P.A.; Chirvony, V.S.; Kvach, V.V.; Orlovich, V.A., Resonance Raman, CARS, and Picosecond Absorption-Spectroscopy of Copper Porphyrins - The Evidence for the Exciplex Formation with Oxygen-Containing Solvent Molecules. *J. Phys. Chem.* **1995,** 99, 2978–2995, https://10.1021/j100010a006.
34. Kim, D.H.; Holten, D.; Gouterman, M., A Picosecond Study of Rapid Excited-State Relaxation via Charge-Transfer States in Ligated Cu(II) Porphyrins. *J. Am. Chem. Soc.* **1984,** 106, 2793–2798.
35. Zhang, Z.Q.; Duan, Y.; Zhang, L.; Yu, M.M.; Li, J., Synthesis, crystal structure of two new Zn(II), Cu(II) porphyrins and their catalytic activities to ethylbenzene oxidation. *Inorg. Chem. Commun.* **2015,** 58, 53–56, https://10.1016/j.inoche.2015.05.024.
36. Kuramochi, Y.; Hashimoto, S.; Kawakami, Y.; Asano, M.S.; Satake, A., Visualization of nonemissive triplet species of Zn(II) porphyrins through Cu(II) porphyrin emission via the reservoir mechanism in a porphyrin macroring. *Photochemical & Photobiological Sciences* **2018,** 17, 883–888, https://10.1039/c8pp00210j.
37. AsanoSomeda, M.; Ichino, T.; Kaizu, Y., Triplet-triplet intramolecular energy transfer in a covalently linked copper(II) porphyrin-free base porphyrin hybrid dimer: A time-resolved ESR study. *J. Phys. Chem. A* **1997,** 101, 4484–4490, https://10.1021/jp962634r.
38. Dong, Z.C.; Kar, A.; Dorozhkin, R.; Amemiya, K.; Uchihashi, T.; Yokoyama, S.; Kamikado, I.; Mashiko, S.; Okamoto, T., Tunneling electron induced luminescence from monolayered Cu-TBP porphyrin molecules adsorbed on Cu(100). *Thin Solid Films* **2003,** 438, 262–267, https://10.1016/s0040-6090(03)00797-1.
39. Ivashin, N.V.; Terekhov, S.N., Resonance Raman Scattering Spectra of Co(II)- and Cu-5,10,15,20-Tetrakis 4-(N-methylpyridyl) porphyrin in the dd Excited State and Mechanisms of Its Deactivation in a Solution and in Complexes with DNA. *Opt. Spectrosc.* **2020,** 128, 1768–1777, https://10.1134/s0030400x20110132.
40. Shvedko, A.G.; Kruglik, S.G.; Ermolenkov, V.V.; Orlovich, V.A.; Turpin, P.Y.; Greve, J.; Otto, C., Mechanism of exciplex formation between Cu-porphyrin and calf-thymus DNA as revealed by saturation resonance Raman spectroscopy. *J. Raman Spec.* **1999,** 30, 677–684, https://10.1002/(sici)1097-4555(199908)30:8<677::aid-jrs440>3.0.co;2-9.
41. Chirvony, V.S.; Negrerie, M.; Martin, J.-L.; Turpin, P.-Y., Picosecond Dynamics and Mechanisms of Photoexcited Cu(II)-5,10,15,20-meso-tetrakis(4-N-methylpyridyl)porphyrin Quenching by Oxygen-Containing Lewis-Base Solvents. *J. Phys. Chem. A* **2002,** 106, 5760–5767, https://10.1021/jp0134998.
42. Inamo, M.; Aoki, K.; Ono, N.; Takagi, H.D., Electron transfer reaction of Cu(II) porphyrin complex: Effect of structural deformation on the electron self-exchange rate. *Inorg. Chem. Commun.* **2005,** 8, 979–982, https://10.1016/j.inoche.2005.07.022.
43. Li, R.L.; Yuan, Y.Q.; Liang, L.; Lu, J.F.; Cui, C.X.; Niu, H.Y.; Wu, Z.R.; Liu, G.C.; Hu, Z.C.; Xie, R.H.; Huang, F.; Zhang, Y.P., Cu(ii)-Porphyrin based near-infrared molecules: synthesis, characterization and photovoltaic application. *New J. Chem.* **2021,** 45, 1601–1608, https://10.1039/d0nj04800c.
44. Venkatesh, B.; Hori, H.; Miyazaki, G.; Nagatomo, S.; Kitagawa, T.; Morimoto, H., Coordination geometry of Cu-porphyrin in Cu(II)-Fe(II) hybrid hemoglobins studied by Q-band EPR and resonance Raman spectroscopies. *J. Inorg. Biochem.* **2002,** 88, 310–315, https://10.1016/s0162-0134(01)00391-9.

45. Jeong, D.; Kang, D.-g.; Joo, T.; Kim, S.K., Femtosecond-Resolved Excited State Relaxation Dynamics of Copper (II) Tetraphenylporphyrin (CuTPP) After Soret Band Excitation. *Scientific Reports* **2017,** 7, 1–8, https://DOI:10.1038/s41598-017-17296-z.
46. Wang, X.Q.; Li, S.Y.; Zhao, L.; Xu, C.M.; Gao, J.S., A DFT and TD-DFT study on electronic structures and UV-spectra properties of octaethyl-porphyrin with different central metals (Ni, V, Cu, Co). *Chin. J. Chem. Eng.* **2020,** 28, 532–540, https://10.1016/j.cjche.2019.07.008.
47. Atanasov, M.; Daul, C.A.; Rohmer, M.M.; Venkatachalam, T., A DFT based ligand field study of the EPR spectra of Co(II) and Cu(II) porphyrins. *Chem. Phys. Lett.* **2006,** 427, 449–454, https://10.1016/j.cplett.2006.06.107.
48. Sorgues, S.; Poisson, L.; Raffael, K.; Krim, L.; Soep, B.; Shafizadeh, N., Femtosecond electronic relaxation of excited metalloporphyrins in the gas phase. *J. Chem. Phys.* **2006,** 124, https://10.1063/1.2176612.
49. Liu, F.; Cunningham, K.L.; Uphues, W.; Fink, G.W.; Schmolt, J.; McMillin, D.R., Luminescence Quenching of Copper(II) Porphyrins with Lewis Bases. *Inorg. Chem.* **1995,** 34, 2015–2018, https://10.1021/ic00112a011.
50. Kim, D.; Holten, D.; Gouterman, M., Evidence from Picosecond Transient Absorption and Kinetic-Studies of Charge-Transfer States in Copper(II) Porphyrins. *J. Am. Chem. Soc.* **1984,** 106, 2793–2798, https://10.1021/ja00322a012.
51. de Paula, J.C.; Walters, V.A.; Jackson, B.A.; Cardozo, K., Transient Resonance Raman Spectroscopy of Copper(II) Complexes of *meso*-Tetraphenylporphine and *meso*-Tetraphenylchlorin. *J. Phys. Chem.* **1995,** 99, 4373–4379, https://10.1021/j100013a004.
52. Jeoung, S.C.; Kim, D.H.; Cho, D.W.; Yoon, M.J., Time-Resolved Resonance Raman Spectroscopic Study on Copper(II) Porphyrin in Various Solvents: Solvent Effects on the Charge-Transfer States. *J. Phys. Chem.* **1995,** 99, 5826–5833, https://10.1021/j100016a016.
53. Jeoung, S.C.; Eom, H.S.; Kim, D.; Cho, D.W.; Yoon, M., Exciplex formation dynamics of photoexcited copper(II) tetrakis(4-N-methylpyridyl)porphyrin with synthetic polynucleotides probed by transient absorption and Raman spectroscopic techniques. *J. Phys. Chem. A* **1997,** 101, 5412–5417, https://10.1021/jp970983v.
54. Mojzes, P.; Chinsky, L.; Turpin, P.Y., Interaction of Electronically Excited Copper(II) Porphyrin with Oligonucleotides and Polynucleotides - Exciplex Building Process by Photoinitiated Axial Ligation of Porphyrin to Thymine and Uracil Residues. *J. Phys. Chem.* **1993,** 97, 4841–4847, https://10.1021/j100120a042.
55. Mojzes, P.; Kruglik, S.G.; Baumruk, V.; Turpin, P.Y., Interactions of electronically excited Copper(II)-porphyrin with DNA: resonance Raman evidence for the exciplex formation with adenine and cytosine residues. *J. Phys. Chem. B* **2003,** 107, 7532–7535, https://10.1021/jp034677v.
56. Kruglik, S.G.; Galievsky, V.A.; Chirvony, V.S.; Apanasevich, P.A.; Ermolenkov, V.V.; Orlovich, V.A.; Chinsky, L.; Turpin, P.Y., Dynamics and Mechanism of the Exciplex Formation Between Cu(TMPY-P4) and DNA Model Compounds Revealed by Time-Resolved Transient Absorption and Resonance Raman Spectroscopies. *J. Phys. Chem.* **1995,** 99, 5732–5741, https://10.1021/j100015a066.
57. Hudson, B.P.; Sou, J.; Berger, D.J.; D.R., M., Luminescence Studies of the Intercalation of Cu(TMpyP4) into DNA. *J. Am. Chem. Soc.* **1992,** 114, 8997–9002.
58. Miller, J.R.; Dorough, G.D., Pyridinate Complexes of some Metallo-Derivatives of Tetraphenylporphine and Tetraphenylchlorin. *J. Am. Chem. Soc.* **1952,** 74, 3977–3981, https://10.1021/ja01136a003.
59. Ha-Thi, M.H.; Shafizadeh, N.; Poisson, L.; Soep, B., An Efficient Indirect Mechanism for the Ultrafast Intersystem Crossing in Copper Porphyrins. *J. Phys. Chem. A* **2013,** 117, 8111–8118, https://10.1021/jp4008015.
60. Lipscomb, L.A.; Zhou, F.X.; Presnell, S.R.; Woo, R.J.; Peek, M.E.; Plaskon, R.R.; Williams, L.D., Structure of a DNA - Porphyrin complex. *Biochemistry* **1996,** 35, 2818–2823, https://10.1021/bi952443z.
61. Rodriguez, J.; Kirmaier, C.; Holten, D., Optical-Properties of MetalloPorphyrin Excited-States. *J. Am. Chem. Soc.* **1989,** 111, 6500–6506, https://10.1021/ja00199a004.
62. Frisch, M.J.; Trucks, G.W.; Schlegel, H.B.; Scuseria, G.E.; Robb, M.A.; Cheeseman, J.R.; Scalmani, G.; Barone, V.; Petersson, G.A.; Nakatsuji, H.; Li, X.; Caricato, M.; Marenich, A.V.; Bloino, J.; Janesko, B.G.; Gomperts, R.; Mennucci, B.; Hratchian, H.P.; Ortiz, J.V.; Izmaylov, A.F.; Sonnenberg, J.L.; Williams-Young, D.; Ding, F.; Lipparini, F.; Egidi, F.; Goings, J.; Peng, B.; Petrone, A.; Henderson, T.; Ranasinghe, D.; Zakrzewski, V.G.; Gao, J.; Rega, N.; Zheng, G.; Liang, W.; Hada, M.; Ehara, M.; Toyota, K.; Fukuda, R.; Hasegawa, J.; Ishida, M.; Nakajima, T.; Honda, Y.; Kitao, O.; Nakai, H.; Vreven, T.; Throssell, K.; Montgomery, J.A.; Peralta, J.E.; Ogliaro, F.; Bearpark, M.J.; Heyd, J.J.; Brothers, E.N.; Kudin, K.N.; Staroverov, V.N.; Keith, T.A.; Kobayashi, R.; Normand, J.; Raghavachari, K.; Rendell, A.P.; Burant, J.C.; Iyengar, S.S.; Tomasi, J.; Cossi, M.; Millam, J.M.; Klene, M.; Adamo, C.; Cammi, R.; Ochterski, J.W.; Martin, R.L.; Morokuma, K.; Farkas, O.; Foresman, J.B.; Fox, D.J., Gaussian 16. **2016**.
63. Becke, A.D., Density-Functional Thermochemistry 3. The Role of Exact Exchange. *J. Chem. Phys.* **1993,** 98, 5648–5652, https://10.1063/1.464913.
64. Lee, C.T.; Yang, W.T.; Parr, R.G., Development of the Colle-Salvetti Correlation-Energy Formula into a Functional of the Electron-Density. *Phys. Rev. B* **1988,** 37, 785–789, https://10.1103/physrevb.37.785.

65. Dunning Jr, T.H.; Hay, P.J., Modern Theoretical Chemistry. In *Modern Theoretical Chemistry*, Schaefer III, H.F., Ed. Plenum Press: New York, 1977; Vol. 3.
66. Hay, P.J.; Wadt, W.R., Ab Initio Effective Core Potentials for Molecular Calculations - Potentials for the Transition-Metal Atoms Sc to Hg. *J. Chem. Phys.* **1985,** 82, 270–283.
67. Hay, P.J.; Wadt, W.R., Ab Initio Effective Core Potentials for Molecular Calculations - Potentials for K to Au Including the Outermost Core Orbitals. *J. Chem. Phys.* **1985,** 82, 299–310.
68. Bauernschmitt, R.; Ahlrichs, R., Treatment of electronic excitations within the adiabatic approximation of time dependent density functional theory. *Chem. Phys. Lett.* **1996,** 256, 454–464, https://10.1016/0009-2614(96)00440-X.
69. Casida, M.E.; Jamorski, C.; Casida, K.C.; Salahub, D.R., Molecular excitation energies to high-lying bound states from time-dependent density-functional response theory: Characterization and correction of the time-dependent local density approximation ionization threshold. *J. Chem. Phys.* **1998,** 108, 4439–4449, https://10.1063/1.475855.
70. Stratmann, R.E.; Scuseria, G.E.; Frisch, M.J., An efficient implementation of time-dependent density-functional theory for the calculation of excitation energies of large molecules. *J. Chem. Phys.* **1998,** 109, 8218–8224, https://10.1063/1.477483.
71. Van Caillie, C.; Amos, R.D., Geometric derivatives of excitation energies using SCF and DFT. *Chem. Phys. Lett.* **1999,** 308, 249–255.
72. Furche, F.; Ahlrichs, R., Adiabatic time-dependent density functional methods for excited state properties. *J. Chem. Phys.* **2002,** 117, 7433–7447.
73. Scalmani, G.; Frisch, J.; Mennucci, B.; Tomasi, J.; Cammi, R.; Barone, V., Geometries and properties of excited states in the gas phase and in solution: Theory and application of a time-dependent density functional theory polarizable continuum model. *J. Chem. Phys.* **2006,** 124, 094107–14.
74. Cossi, M.; Barone, V.; Cammi, R.; Tomasi, J., Ab initio study of solvated molecules: A new implementation of the polarizable continuum mode. *Chem. Phys. Lett.* **1996,** 255, 327–335, https://10.1016/0009-2614(96)00349-1.
75. Tomasi, J.; Mennucci, B.; Cammi, R., Quantum mechanical continuum solvation models. *Chem. Rev.* **2005,** 105, 2999–3093, https://10.1021/cr9904009.
76. Dennington II, R.D.; Keith, T.A.; Millam, J.M. *GaussView*, Semichem, Inc.: 2016.